electronic reprint

Acta Crystallographica Section B
Structural Science
ISSN 0108-7681
Editor: **Carolyn P. Brock**

Order–disorder character and twinning in the structure of a new synthetic titanosilicate: $(Ba,Sr)_4Ti_6Si_4O_{24}\cdot H_2O$

Marcella Cadoni, Andrea Bloise, Giovanni Ferraris and Stefano Merlino

Acta Cryst. (2008). B**64**, 669–675

Copyright © International Union of Crystallography

Author(s) of this paper may load this reprint on their own web site or institutional repository provided that this cover page is retained. Republication of this article or its storage in electronic databases other than as specified above is not permitted without prior permission in writing from the IUCr.

For further information see http://journals.iucr.org/services/authorrights.html

Acta Crystallographica Section B: Structural Science publishes papers in structural chemistry and solid-state physics in which structure is the primary focus of the work reported. The central themes are the acquisition of structural knowledge from novel experimental observations or from existing data, the correlation of structural knowledge with physicochemical and other properties, and the application of this knowledge to solve problems in the structural domain. The journal covers metals and alloys, inorganics and minerals, metal-organics and purely organic compounds.

Crystallography Journals Online is available from **journals.iucr.org**

Acta Crystallographica Section B
Structural Science
ISSN 0108-7681

Order–disorder character and twinning in the structure of a new synthetic titanosilicate: $(Ba,Sr)_4Ti_6Si_4O_{24}\cdot H_2O$

Marcella Cadoni,[a] Andrea Bloise,[a,b] Giovanni Ferraris[a]* and Stefano Merlino[c]

[a]Dipartimento di Scienze Mineralogiche e Petrologiche, Università di Torino, Via Valperga Caluso 35, 10125 Torino, Italy, [b]Dipartimento di Scienze della Terra, Università della Calabria, Via Pietro Bucci, 87036 Arcavacata di Rende (CS), Italy, and [c]Dipartimento di Scienze della Terra, Università di Pisa, Via S. Maria 53, 56126 Pisa, Italy

Correspondence e-mail: giovanni.ferraris@unito.it

Received 30 June 2008
Accepted 9 October 2008

Prismatic crystals of the title compound, up to 100 μm long and {001} twinned by metric merohedry, were obtained as a side-product of a hydrothermal run devoted to synthesizing the heterophyllosilicate lamprophyllite. Single-crystal X-ray diffraction data were collected on a Bruker-AXS Smart Apex diffractometer from a crystal with approximate composition $(Ba_{0.80}Sr_{0.20})_4Ti_6Si_4O_{24}\cdot H_2O$. The structure was solved and refined as a disordered structure in the space group *Cmmm* [a_o = 5.906 (2), b_o = 20.618 (8), c_o = 16.719 (6) Å, R = 0.089 for 682 reflections with $I_o > 2\sigma(I_o)$], and then deciphered by the order–disorder (OD) theory as an ordered structure and refined in the space group $P2/c$ [a = 5.906, b = 16.719, c = 10.724 Å, β = 105.99°, R = 0.083 for 1090 reflections with $I_o > 2\sigma(I_o)$]. The discussion based on the OD theory shows that the refined ordered structure corresponds to one (2*M*) of two maximum degree of order (MDO) polytypes. The structure of the second MDO polytype (4*O*) was modelled but not refined because it does not substantially occur in our sample. In the structure, infinite (001) ribbons of Ti octahedra elongated along the [100] direction are connected by $(SiO_3)_4$ four-membered rings, thus realising a new type of heteropolyhedral framework. The ribbons are three-octahedra wide and one-octahedron thick; they are formed by linking, *via* edge-sharing, rutile-type edge-sharing rows of octahedra. This ribbon represents a slice of the octahedral sheet that occurs in perrierite-(Ce), $Ce_4MgFe_2Ti_2O_8(Si_2O_7)_2$. The (Ba,Sr) ions are hosted within two independent [100] narrow channels both delimited by four Ti octahedra and four Si tetrahedra. The disorder of H_2O is discussed on the basis of a Raman spectrum.

1. Introduction

Titanosilicates have attracted much interest in recent years because of their potentially important technological properties (ion-exchange, sorption, catalysis *etc.*). They include a variety of types of new crystal structures that have often been first studied in natural minerals and then have been reproduced, with variants, in the laboratory during the search for new materials (for a recent review see Ferraris & Merlino, 2005).

As a side-product of a hydrothermal run devoted to synthesizing the layered heterophyllosilicate (*cf.* Ferraris, 2008) lamprophyllite, ideally $Na_3(SrNa)Ti_3(Si_2O_7)_2O_2(OH)_2$, we obtained prismatic crystals of $(Ba,Sr)_4Ti_6Si_4O_{24}\cdot H_2O$ (abbreviated as TR02). In view of the interest in titanosilicates mentioned above, this article describes the synthesis and the crystal structure of TR02. At the same time, the structure offers a paradigmatic example of applying the OD theory to decipher the structural disorder and related appearance of

© 2008 International Union of Crystallography
Printed in Singapore – all rights reserved

electronic reprint

twinning (for a detailed review of both these topics, see Ferraris *et al.*, 2008).

1.1. OD theory

OD structures built from equivalent layers occur when the layers may stack according to $Z > 1$ geometrically equivalent modes. The various disordered or ordered sequences of Z stacking modes give rise to a family of infinite disordered or ordered structures (polytypes): pairs of adjacent layers are geometrically equivalent in all the structures of the family. The common symmetry properties of the whole family are fully described by giving the λ operations (symmetry operations of the single layer, forming one of the 80 layer groups) and the σ operations, namely the set of operations converting a layer into the next one. All these coincidence operations are generally only valid in a subspace of the crystal space and are therefore indicated as 'partial operations' (POs).

The derivation of the sets of σ operations that are compatible with the symmetry of each layer group was one of the most important results of the OD theory (Dornberger-Schiff, 1964). The knowledge of these sets is extremely helpful in deriving the symmetry of particular ordered sequences and in dealing with the diffraction aspects of the whole family. In fact, all disordered and ordered members of the OD family present a common set of reflections (family reflections), whereas they can be distinguished on the basis of additional 'characteristic' (non-family) reflections. The family reflections correspond to a fictitious structure, periodic in three dimensions, closely related to the structures of the family and called family structure (more loosely indicated as the average structure). It may be obtained from any polytype of the family, by superposing Z copies of it translated by the vector (or vectors) corresponding to the possible Z positions of each OD layer. Whereas the family reflections are always sharp, the characteristic reflections may be sharp, as well as more or less diffuse, sometimes appearing as continuous streaks running along the stacking direction. Often it is just the presence of diffuse reflections, together with non-space-group systematic absences, which points to the OD character of the phase under study.

Another important result of the OD theory is the definition of the concept of structures of the maximum degree of order (MDO structures) as those sequences in which not only pairs, but also triples, quadruples *etc.* of layers are geometrically equivalent, as far as possible (a detailed definition may be found in Dornberger-Schiff, 1964, and in Ferraris *et al.*, 2008): MDO structures correspond to the most frequently occurring polytypes in the family, often called 'simple' or 'regular'.

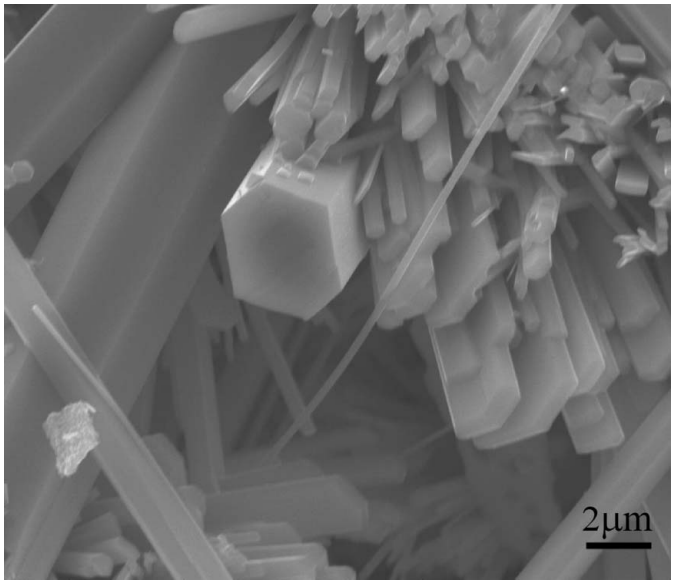

Figure 1
SEM image showing the prismatic morphology of TR02 corresponding to the three larger crystals on the left side. The bundle of smaller crystals corresponds to matsubaraite.

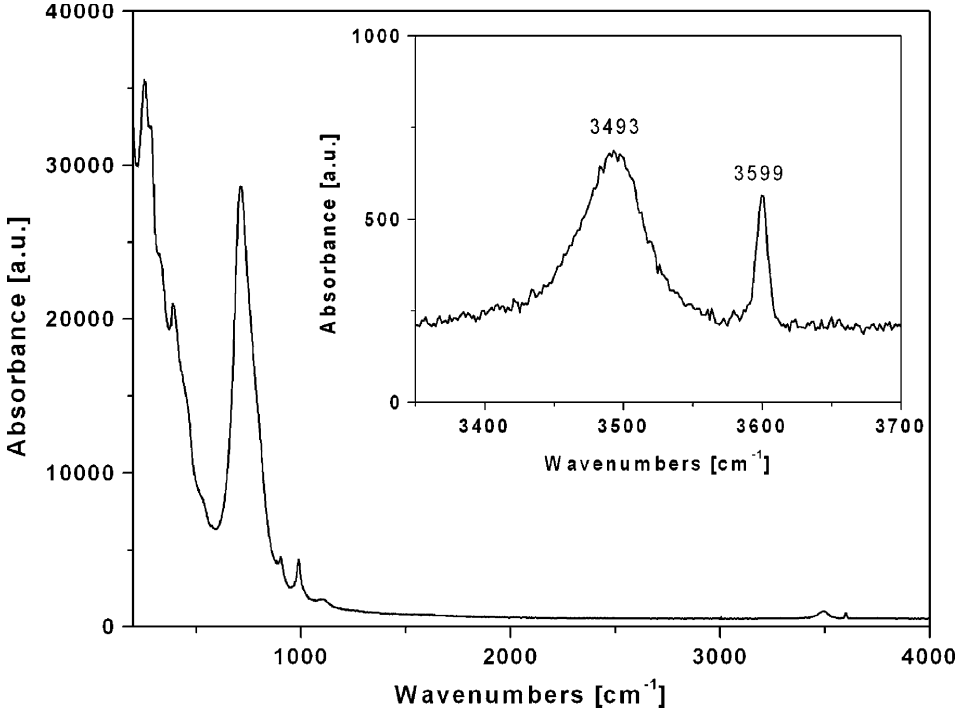

Figure 2
Raman spectrum of TR02. The inset shows the part of the spectrum related to the OH stretching of H_2O.

2. Experimental

2.1. Synthesis of $(Ba,Sr)_4Ti_6Si_4O_{24}\cdot H_2O$

About 70 mg of finely (< 0.18 mm) powdered chemicals plus water (8% weight), according

electronic reprint

Table 1
Experimental details.

	Disordered structure	2*M* polytype
Crystal data		
Chemical formula	$(Ba,Sr)_4Ti_6Si_4O_{24}\cdot H_2O$	$Ba_{3.20}O_{24}Si_4Sr_{0.80}Ti_6\cdot H_2O$
M_r	1351.14	1311.36
Cell setting, space group	Orthorhombic, *Cmmm*	Monoclinic, *P*2/*c*
Temperature (K)	293 (2)	293 (2)
a, *b*, *c* (Å)	5.906 (2), 20.618 (8), 16.719 (6)	5.906 (2), 16.719 (6), 10.724 (5)
β (°)	90.00	105.99 (5)
V (Å^3)	2035.9 (13)	1017.9 (7)
Z	4	2
D_x (Mg m^{-3})	4.408	4.343
Radiation type	Mo $K\alpha$	Mo $K\alpha$
μ (mm^{-1})	10.18	10.46
Crystal form, colour	Prismatic, opaque grey	Prismatic, opaque grey
Crystal size (mm)	0.13 × 0.01 × 0.01	0.13 × 0.01 × 0.01
Data collection		
Diffractometer	Bruker Smart Apex	Bruker Smart Apex
Data collection method	φ/ω	φ/ω
Absorption correction	Multi-scan†	Multi-scan†
T_{min}	0.363	0.355
T_{max}	0.905	0.903
No. of measured, independent and observed reflections	10 044, 1411, 692	10 045, 2476, 1089
Criterion for observed reflections	$I > 2\sigma(I)$	$I > 2\sigma(I)$
R_{int}	0.339	0.198
θ_{max} (°)	27.9	27.9
Refinement		
Refinement on	F^2	F^2
$R[F^2 > 2\sigma(F^2)]$, $wR(F^2)$, S	0.089, 0.239, 1.04	0.083, 0.227, 0.96
No. of reflections	1411	2476
No. of parameters	96	99
H-atom treatment	Mixture‡	Mixture
Weighting scheme	$w = 1/[\sigma^2(F_o^2) + (0.0966P)^2]$, where $P = (F_o^2 + 2F_c^2)/3$	$w = 1/[\sigma^2(F_o^2) + (0.1034P)^2]$, where $P = (F_o^2 + 2F_c^2)/3$
$(\Delta/\sigma)_{max}$	< 0.0001	0.786
$\Delta\rho_{max}$, $\Delta\rho_{min}$ (e Å^{-3})	3.70, −4.12	2.87, −2.79
Extinction method	*SHELXL*	*SHELXL*
Extinction coefficient	0.0015 (2)	0.0039 (6)

Computer programs used: *SHELXL*97, *SHELXS*97 (Sheldrick, 2008), *ATOMS*6.2 (Dowty, 2002). † Based on 8 symmetry-related measurements. ‡ Mixture of independent and constrained refinement.

to an $Na_2Sr_{1.3}Ba_{0.7}Ti_3Si_4O_{16}(OH)_2$ stoichiometry suitable to obtain a lamprophyllite-like compound, were sealed within a platinum capsule (0.11 cm^3 in volume). The synthesis was carried out for 1 week in an externally heated pressure vessel at 673 K, 1 kbar, under alkaline conditions obtained by the addition of NaF + NaOH (pH = 9). Finally, the capsule was rapidly quenched in water. The following chemicals with purity higher than 98% were used: quartz converted to cristobalite by heating at 1673 K; titania gel prepared from $TiCl_4$ (Kolen'ko *et al.*, 2004), NaOH, NaF, BaO and SrO. All chemicals were from Carlo Erba, except BaO and SrO which were from Sigma-Aldrich. Identified crystalline phases (Fig. 1) are TR02 (length of the prismatic crystals up to 100 µm), matsubaraite, $Sr_4Ti_5O_8(Si_2O_7)_2$, and benitoite, $BaTiSi_3O_9$. Wave-dispersive spectroscopy (WDS) electron microprobe analyses (Jeol JXA 8200) showed inhomogeneous crystals whose chemical composition is variable in Ba and Sr content (0.7 < Ba/Sr < 4.0) according to a linear correlation. Crystal zoning and crystals with different compositions are indicative of crystallization under non-equilibrium conditions.

2.2. Diffraction and Raman data collection

Single-crystal X-ray diffraction data for TR02 were collected on a Bruker-AXS Smart Apex diffractometer under the experimental conditions shown in Table 1[1] and according to an orthorhombic cell with a_o = 5.906 (2), b_o = 20.618 (8), c_o = 16.719 (6) Å. The refinement of the cell parameters was based on all measured reflections with $I_o > 10\sigma(I_o)$.

A Raman spectrum (Fig. 2) was collected by a LabRam HR800 micro-Raman spectrometer (Jobin Yvon) equipped with a HeNe laser at an excitation wavelength of 562 nm, a CCD detector and an Olympus BX41 optical microscope.

3. Results

3.1. Structure solution and refinement

The analysis of the reflections indexed in the orthorhombic cell given above shows that:

(i) the value of R_{int} = 0.34 for the point group *mmm* is higher than the value for the point group 112/*m* (R_{int} = 0.20);

(ii) non-space-group absences of the reflections with $2h + 2k + l = 2n + 1$ occur.

In spite of the higher R_{int} value, a reasonable solution (direct methods) and refinement (R = 0.089) of the structure could be obtained only in the space group *Cmmm* (supplementary material). Only some of the atoms have been anisotropically refined (supplementary material). The structure shows disorder in the sites Ba2, Si1, Si2, O12 and O*W*2 (supplementary material, Fig. 3) that are only 50% occupied. The disorder is concentrated within a (001) slab that is $c_o/2$ thick (c_o refers to the *Cmmm* cell) and alternates along [001] with an analogous ordered slab. Actually, apart from the disorder that is consequent to twinning (see below), the two types of slab are equivalent according to a situation recently observed in vurroite, $Pb_{20}Sn_2(Bi,As)_{22}S_{54}Cl_6$, whose real structure has

[1] Supplementary data for this paper are available from the IUCr electronic archives (Reference: CK5034). Services for accessing these data are described at the back of the journal.

electronic reprint

been defined through the application of the OD theory (Pinto *et al.*, 2008). In fact, as discussed below, adjacent layers are related by one of the two stacking vectors $\mathbf{t}_1 = \mathbf{c}_o/2 + (\mathbf{a}_o + \mathbf{b}_o)/4$ and $\mathbf{t}_2 = \mathbf{c}_o/2 + (\mathbf{a}_o - \mathbf{b}_o)/4$, both giving rise to pairs of geometrically equivalent layers.

Although no streaking of reflections has been observed (as can be expected in layer-disordered structures), the OD character of TR02 is revealed by the above-mentioned non-space-group absences of the reflections. As discussed in §4.2, it was proved that the disordered structure solved in the space group *Cmmm* is the result of twinning of a *P*2/*c* monoclinic structure with the unit cell defined by the vectors $\mathbf{a} = -\mathbf{a}_o$, $\mathbf{b} = \mathbf{c}_o$, $\mathbf{c} = (\mathbf{a}_o + \mathbf{b}_o)/2$. The corresponding cell parameters are $a = 5.906$, $b = 16.719$, $c = 10.724$ Å, $\beta = 105.99°$. The *P*2/*c* structure corresponds to one (2*M* polytype) of the two MDO polytypes among the infinite polytypes that can be generated by different stacking sequences of the $\mathbf{t}_1$ and $\mathbf{t}_2$ vectors. Precisely, it corresponds to the polytype generated by one of the sequences $\mathbf{t}_1\mathbf{t}_1\mathbf{t}_1 \ldots$ and $\mathbf{t}_2\mathbf{t}_2\mathbf{t}_2 \ldots$; the two structures are related by twinning by metric merohedry (Nespolo & Ferraris, 2000), twin plane (001) [monoclinic reference; (010) in the orthorhombic reference]. The possibility of twinning by metric merohedry may be easily understood if one takes into account that actually the lattice of the monoclinic structure is metrically o*C*, as shown by the orthorhombic cell used to describe the disordered structure.

The ordered structure model generated by the action of $\mathbf{t}_1$ on the $c_o/2$ thick (001) slab (Fig. 4) was refined to $R = 0.083$, including the 'TWIN 100 010 −10–1' instruction to account for a possible (001) twin by metric merohedry as mentioned above. In fact, the presence of two twinned individuals in the ratio 4:1 was revealed. The resulting atom parameters and displacements are given in the supplementary material. Only the Ba and Ti atoms were anisotropically refined (supplementary material). The ordered refinement in *P*2/*c* converges to an *R* value only slightly lower than that obtained in the refinement of the *Cmmm* disordered structure, and in both cases only a partial anisotropic refinement can be carried out. The highest positive and negative residual peaks in the electron-density difference map (Table 1; 2*M* polytype) are close to Ti1 (0.60 Å) and Ba1 (0.90 Å), respectively. These and other problems with the refinement, the high e.s.d.s on the atom coordinates and the high *R* values, can be related to at least three aspects:

(i) absorption correction based on pseudo-equivalent orthorhombic reflections (the correction based on the crystal shape was even worse);

(ii) the very small size of the crystal used, with consequent low scattering power (only about 50% of reflections were observed);

(iii) a likely presence of disordered polytypic sequences.

The latter aspect is common in OD crystal structures because OD character in fact implies some stacking disorder (see *e.g.* the already quoted case of vurroite). The presence of substantial domains of the second MDO polytype (see §4.2) with cell parameters $a' = a_o = 5.906$, $b' = b_o = 20.618$, $c' = 2c_o = 33.438$ Å and space group *Fddd* is ruled out by the absence of observed reflections pointing to the presence of the long cell parameter $c' = 2c_o$. The atom coordinates of the model built for the *Fddd* structure (4*O* polytype, Fig. 5) are given in the supplementary material.

To take into account that (§4.2), as previously indicated, the family reflections (*h* even, and also *k* even, due to the *C* centring of the single OD layer) are common to all ordered and disordered sequences and are sharp, whereas non-family (*h* and *k* odd) reflections receive contributions only from the

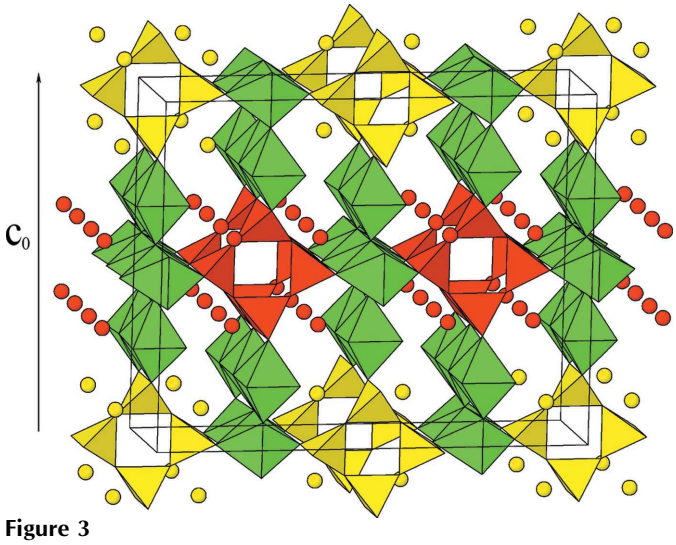

Figure 3
Disordered structure of TR02 in *Cmmm*; as seen approximately down $\mathbf{a}_o$; the disordered part is shown in red. Yellow and red circles represent (Ba,Sr) ions. H_2O molecules are sandwiched between two four-membered rings and are not shown. This figure is in colour in the electronic version of this paper.

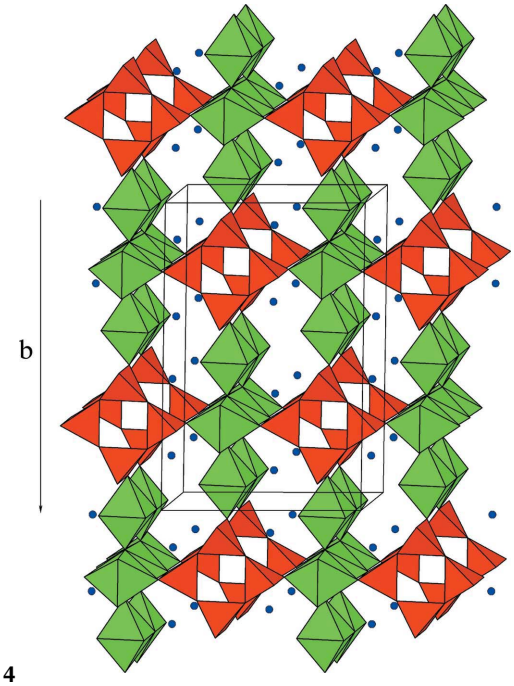

Figure 4
Refined structure of the ordered 2*M* polytype as seen approximately down **a**. Blue circles represent (Ba,Sr) ions. H_2O molecules are sandwiched between two four-membered rings and are not shown. This figure is in colour in the electronic version of this paper.

electronic reprint

Table 2
Important bond distances for the 2*M* polytype.

Ti1—O3 2×	1.91 (3)	Ba1—O8	2.64 (4)
Ti1—O4 2×	2.02 (3)	Ba1—O6	2.65 (3)
Ti1—O11 2×	2.02 (2)	Ba1—O9	2.65 (3)
Ti2—O5	1.77 (4)	Ba1—O11	2.80 (4)
Ti2—O7	1.86 (4)	Ba1—O9	2.80 (3)
Ti2—O10	2.00 (3)	Ba1—O*W*	2.87 (5)
Ti2—O3	2.02 (3)	Ba1—O12	2.88 (4)
Ti2—O5	2.07 (4)	Ba1—O6	2.93 (3)
Ti2—O7	2.09 (4)	Ba1—O4	3.03 (2)
Ti3—O4 2×	1.92 (3)	Ba1—O1	3.08 (3)
Ti3—O12 2×	2.00 (2)	Ba1—O1	3.13 (4)
Ti3—O3 2×	2.06 (3)	Ba2—O7	2.61 (4)
Ti4—O6	1.83 (3)	Ba2—O10	2.68 (3)
Ti4—O8	1.91 (4)	Ba2—O5	2.71 (4)
Ti4—O4	2.04 (2)	Ba2—O11	2.84 (4)
Ti4—O9	2.05 (3)	Ba2—O12	2.85 (4)
Ti4—O6	2.08 (3)	Ba2—O10	2.86 (3)
Ti4—O8	2.15 (4)	Ba2—O*W*	2.96 (5)
Si1—O9 2×	1.63 (3)	Ba2—O5	3.06 (3)
Si1—O1 2×	1.65 (3)	Ba2—O2	3.09 (3)
Si2—O2	1.60 (3)	Ba2—O3	3.21 (3)
Si2—O11	1.61 (2)	Ba2—O2	3.26 (3)
Si2—O12	1.61 (2)	Si2—O1	1.63 (3)
Si3—O10 2×	1.61 (3)	Si3—O2 2×	1.62 (3)

specific structure under study and may be streaked, the two groups of reflections were allowed to have independent scale factors ('Ďurovič effect'; Nespolo & Ferraris, 2001). The refinement of the Ba *versus* Sr content shows that both sites indicated as Ba in the supplementary material have a mixed (Ba,Sr) composition. Whereas in the disordered structure the two Ba sites show the same Ba/Sr ratio (supplementary material), in the 2*M* polytype Sr slightly prefers the Ba1 site (supplementary material). On average, the crystal used for the structure determination has the approximate composition $(Ba_{0.80}Sr_{0.20})_4Ti_6Si_4O_{24}\cdot H_2O$.

4. Structural aspects

4.1. The structure

Selected bond lengths and angles for TR02, calculated in the monoclinic cell with the atom coordinates in the supplementary material, are reported in Table 2. Owing to the high e.s.d.s of the positional parameters, the bond lengths show e.s.d.s of *ca* 0.03 Å such that apparently anomalous bond lengths, such as Ti2—O5 = 1.77 Å, approach normal values within 3 e.s.d.s; no discussion intended to justify bond lengths on a crystal-chemical basis was therefore attempted. Ti and Si show the usual six- and fourfold coordination, respectively; the large alkali ions show 11-fold coordination and quite a distorted polyhedron.

O*W* is the most underbonded oxygen atom in the structure, being coordinated to only Ba (Table 2); consequently, it must correspond to the O atom of the H_2O molecule shown in the chemical formula. The shortest O*W*···O contact is with O9 (3.35 Å), implying that this molecule does not establish hydrogen bonds. O*W* is probably (partially) disordered around its special 2(*e*) position, a situation that would explain the appearance of a sharp and a broad peak at 3599 and 3493 cm^{-1}, respectively, in the OH stretching region of the Raman spectrum (Fig. 2). The sharp and the broad peaks should represent, respectively, the OH stretching frequencies of an H_2O molecule that is distributed between the fixed 2(*e*) site and disordered sites around 2(*e*) to establish a range of weak hydrogen bonds.

In the crystal structure of TR02 infinite (001) ribbons of Ti octahedra, developed along the [100] direction, are connected by $[(SiO_3)_4]^{8-}$ four-membered rings, thus realising a new type of heteropolyhedral framework (indices refer to the monoclinic cell, Fig. 4). Each ribbon is formed by linking, *via* edge-sharing, three rutile-type edge-sharing rows of octahedra. Within each treble-chain ribbon, the shared edges are along [001] in the two lateral rows and along [010] in the central row; thus, the ribbons have a puckered configuration. This type of ribbon is not reported in a recent review of titanosilicates (Sokolova & Hawthorne, 2004) and represents a three-octahedra-wide slice of the octahedral sheet that occurs in perrierite-(Ce), $Ce_4MgFe_2Ti_2O_8(Si_2O_7)_2$ (Gottardi, 1960). The framework is crossed by two independent [100] narrow channels each confined in one *b*/2 layer and hosting, respectively, Ba1 and Ba2; O*W* is instead sandwiched between two four-membered rings. The two channels are very similar and both, as in labuntsovites (*cf.* Cadoni & Ferraris, 2007), are delimited by four Ti octahedra and four Si tetrahedra; however, in the present case, the cross section of the channels is too narrow to classify TR02 as a porous material.

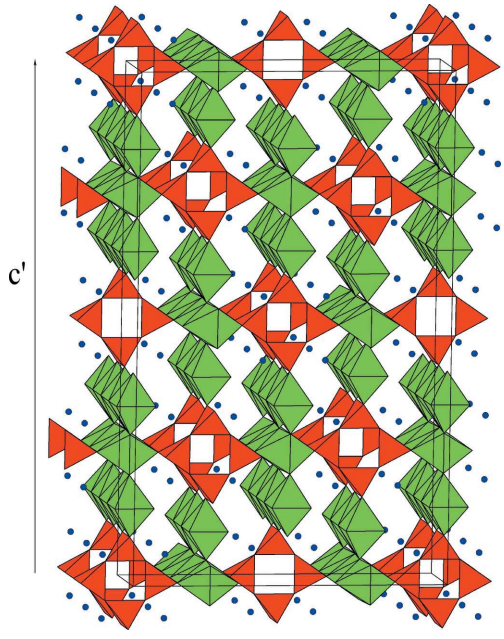

Figure 5
Model structure of the ordered 4*O* polytype, as seen approximately down **a**′. Blue circles represent (Ba,Sr) ions. H_2O molecules are sandwiched between two four-membered rings and are not shown. This figure is in colour in the electronic version of this paper.

electronic reprint

4.2. The OD character

The results of the structural refinement carried out in the space group *Cmmm* gave the following evidence for the OD character of the structure:

(i) regular alternation of ordered layers and disordered layers with atoms distributed on sites with occupancy $\frac{1}{2}$;

(ii) non-space-group systematic absences, in particular reflections with $2h + 2k + l = 2n + 1$. These absences indicate an *I* subcell (family cell, see below; $a_F = a_o/2$, $b_F = b_o/2$, $c_F = c_o$), where the absence rule becomes $H + K + L = 2n + 1$ ($H = 2h$, $K = 2k$, $L = l$).

An examination of the ordered layer gives all the necessary indications about the metrics and the symmetry of the single OD layer. It presents layer symmetry *Cmmm*, with translation vectors $\mathbf{a}_L = \mathbf{a}_o$ and $\mathbf{b}_L = \mathbf{b}_o$ (a_L = 5.906, b_L = 20.618 Å) and a third basic vector (not a translation vector) $\mathbf{c}_L = \mathbf{c}_o/2$ (c_L = 8.359 Å). As already mentioned, the OD theory presents for any layer symmetry the σ operations compatible with it. In the present case we may find (Dornberger-Schiff, 1964; Ferraris *et al.*, 2008)

$$\begin{array}{lcccc} \lambda \text{ operations} & C & m & m & (m) \\ \sigma \text{ operations} & & \{2_r/n_{s,2} & 2_s/n_{2,r} & (2_2/n_{r,s})\}, \end{array} \quad (1)$$

where, as usual in OD theory, the symbols in parentheses refer to the direction of missing periodicity. The results of the refinement in the space group *Cmmm* indicate that $r = s = \frac{1}{2}$.

Adjacent layers are related through the σ operation (σ-PO) $[--n_{1/2,\,1/2}]$ [glide normal to $\mathbf{c}_L$, with translation component $(\mathbf{a}_L + \mathbf{b}_L)/4$] or, because of the λ operation $[-m-]$, through the σ operation $[--n_{1/2,\,-1/2}]$ [glide normal to $\mathbf{c}_L$, with translation component $(\mathbf{a}_L - \mathbf{b}_L)/4$]. Pairs of layers related through one or the other operation are geometrically equivalent; moreover, the layers in both pairs are translationally equivalent and are related by the translations $\mathbf{t}_1 = \mathbf{c}_L + (\mathbf{a}_L + \mathbf{b}_L)/4$ and $\mathbf{t}_2 = \mathbf{c}_L + (\mathbf{a}_L - \mathbf{b}_L)/4$, respectively. Among the infinite possible sequences of the two stacking vectors $\mathbf{t}_1$ and $\mathbf{t}_2$, two correspond to the MDO structures in the family: MDO1, $\mathbf{t}_1\mathbf{t}_1\mathbf{t}_1\mathbf{t}_1\ldots$ and MDO2, $\mathbf{t}_1\mathbf{t}_2\mathbf{t}_1\mathbf{t}_2\ldots$.

Fig. 6 schematically represents the structural arrangement of polytype MDO1, built up as a sequence of layers with *Cmmm* symmetry stacked by the constant application of the vector $\mathbf{t}_1$. The white rhombuses of the figure (actually rhombic prisms in three dimensions with *mmm* symmetry) are located at level 0, whereas the grey rhombuses are located at level 1 (the distance between the two levels is c_L). By applying again the stacking vector $\mathbf{t}_1$, the layer is now placed at level 2; owing to the *C* centring, the layer at level 2 is exactly superimposed to that at level 0, outlining a *C*-centred cell, with basis vectors $\mathbf{a} = \mathbf{a}_L = \mathbf{a}_o$, $\mathbf{b} = \mathbf{b}_L = \mathbf{b}_o$, $\mathbf{c} = 2\mathbf{c}_L = \mathbf{c}_o$. In the figure the structural scheme is seen along $-\mathbf{c}$ (**a** horizontal, **b** vertical). Among the symmetry operations of each layer (2/*m*2/*m*2/*m*), only the operation $[--2]$ is total, being valid for the whole structure. The application of the stacking vector $\mathbf{t}_1$ corresponds, as already said, to the application of the operation $[--n_{1/2,\,1/2}]$, namely a glide $[--d]$. Finally, an inversion centre of σ-type is present, correlating adjacent layers. In conclusion, the MDO1 structure corresponds to the monoclinic polytype 2*M*, with space group *C*112/*d* and cell parameters $a_M = a_o$ = 5.906, $b_M = b_o$ = 20.618, $c_M = c_o$ = 16.719 Å, γ_M = 90.0°. Through the transformation matrix $[\bar{1}00/001/\frac{11}{22}0]$ we may pass from the non-standard *C*112/*d* setting of the space group to its standard *P*12/*c*1 setting used for the structure refinement reported above. As already mentioned, the sequence $\mathbf{t}_2\mathbf{t}_2\mathbf{t}_2\mathbf{t}_2\ldots$ corresponds to the same structure, twin-related to the previous one with the twin plane (001) (indices refer to the *P*2/*c* unit cell).

Fig. 7 schematically represents the structural arrangement of polytype MDO2, built up through the regular alternation of

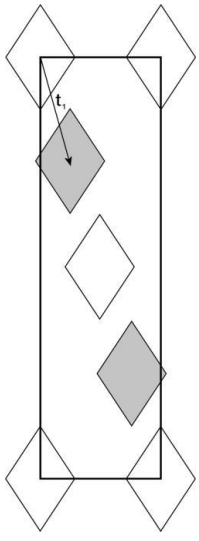

Figure 6
Schematic representation of the layer stacking in the MDO1 polytype represented in the orthorhombic cell of the disordered *Cmmm* structure with cell parameters a_o, b_o and c_o (see text). Projection along $-\mathbf{c}_o$ in the a_ob_o plane ($\mathbf{a}_o$ and $\mathbf{b}_o$ pointing right side and down, respectively).

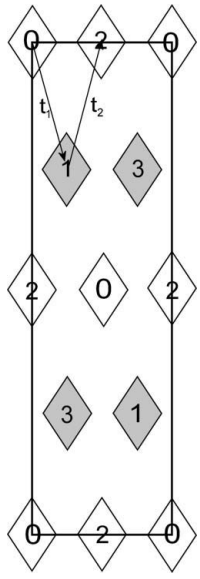

Figure 7
Schematic representation of the layer stacking in the MDO2 polytype. Axes as in Fig. 6.

electronic reprint

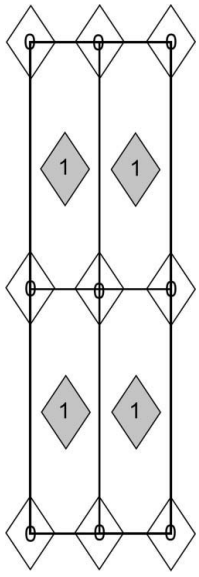

Figure 8
Schematic representation of the family structure; four unit cells projected along $\mathbf{c}_F$ (see text).

the stacking vectors $\mathbf{t}_1$ and $\mathbf{t}_2$. In it the white rhombuses (see Fig. 6) are located at levels 0 and 2, whereas the grey rhombuses are located at levels 1 and 3 (the distance between adjacent levels is c_L). In this way a structure characterized by an *F*-centred cell, with basis vectors $\mathbf{a}' = \mathbf{a}_L = \mathbf{a}_o$, $\mathbf{b}' = \mathbf{b}_L = \mathbf{b}_o$, $\mathbf{c}' = 4\mathbf{c}_L = 2\mathbf{c}_o$, is built up. In the figure the structural scheme is drawn along $\mathbf{c}'$ ($\mathbf{a}'$ horizontal, $\mathbf{b}'$ vertical). The three σ operations $[n_{1/2,2}\,--]$, $[-n_{2,1/2}-]$, $[--\,n_{1/2,1/2}]$ correspond to three glides of type *d* and give rise to the space group *Fddd* (the three twofold rotation axes, which are λ elements of symmetry of the single OD layer, are valid for the whole structure). The MDO2 structure thus corresponds to the orthorhombic polytype 4*O*, with the cell parameters given above.

The family structure may be derived assuming the simultaneous occurrence of both stacking modes. It is schematically represented in Fig. 8 (four adjacent cells are drawn) and presents the space-group symmetry *Immm*, with cell parameters $a_F = a_o/2 = 2.953$, $b_F = b_o/2 = 10.084$, $c_F = c_o = 16.719$ Å [with reference to the parameters of the OD layer $a_F = a_L/2$, $b_F = b_L/2$, $c_F = 2c_L$]. The metrics and symmetry of the family structure are in agreement with the non-space-group absences in the diffraction pattern mentioned above.

5. Conclusions

The application of the OD theory allowed us to decipher the disorder observed in the structure of $(Ba,Sr)_4Ti_6Si_4O_{24}\cdot H_2O$ solved in the *Cmmm* space group according to the cell shown by the X-ray diffraction pattern. Alerted by the occurrence of non-space-group absences, it was shown that this pattern is produced by twinning by metric merohedry of a *P*2/*c* structure representing one (2*M*) of two MDO polytypes that are obtained, respectively, by stacking, according to sequences $\mathbf{t}_1\mathbf{t}_1\mathbf{t}_1\mathbf{t}_1\ldots$ and $\mathbf{t}_1\mathbf{t}_2\mathbf{t}_1\mathbf{t}_2\ldots$, a slice of the disordered structure. The structure of the second polytype (*Fddd*) has been modelled too, but not refined because it was not detected in our crystals.

The structure represents a new type of heteropolyhedral framework with channels delimited by four Ti octahedra and four Si tetrahedra as in minerals of the labuntsovite group; however, in the present case, the channels are quite narrow.

This work was financially supported by MIUR [Roma, project PRIN 2007 'Compositional and structural complexity in minerals (crystal chemistry, microstructures, modularity, modulations): analysis and applications']. We are grateful to Fernando Càmara for assistance in collecting single-crystal data with the Bruker diffractometer of the Istituto di Geoscienze e Georisorse (CNR, Pavia Section). The comments of two anonymous referees helped improve the text.

References

Cadoni, M. & Ferraris, G. (2007). *Eur. J. Mineral.* **19**, 217–222.
Dornberger-Schiff, K. (1964). *Abh. Dtsch. Akad. Wiss.* **3**, 1–107.
Dowty, E. (2002). *ATOMS*, Version 6.2. Shape Software, Kingsport, Tennessee, USA.
Ferraris, G. (2008). *Z. Kristallogr.* **223**, 76–84.
Ferraris, G., Makovicky, E. & Merlino, S. (2008). *Crystallography of Modular Materials.* Oxford University Press.
Ferraris, G. & Merlino, S. (2005). Editors. *Micro- and Mesoporous Mineral Phases.* Washington DC: Mineralogical Society of America, Geochemical Society.
Gottardi, G. (1960). *Am. Mineral.* **45**, 1–14.
Kolen'ko, Yu. V., Burukhin, A. A., Churagulov, B. R. & Oleinikov, N. N. (2004). *Inorg. Mater.* **40**, 822–828.
Nespolo, M. & Ferraris, G. (2000). *Z. Kristallogr.* **215**, 77–81.
Nespolo, M. & Ferraris, G. (2001). *Eur. J. Mineral.* **13**, 1035–1045.
Pinto, D., Bonaccorsi, E., Balić-Žunić, T. & Makovicky, M. (2008). *Am. Mineral.* **93**, 713–727.
Sheldrick, G. M. (2008). *Acta Cryst.* A**64**, 112–122.
Sokolova, E. & Hawthorne, F. C. (2004). *Can. Mineral.* **42**, 807–824.

electronic reprint